



OPEN ACCESS

EDITED BY

Zhan Dou,
Beijing University of Chemical Technology,
China

REVIEWED BY

Qianlin Wang,
Beijing University of Chemical Technology,
China
Lei Ni,
Nanjing Tech University, China

*CORRESPONDENCE

Lijun Wei,
✉ weilj@chinasafety.ac.cn
Yingquan Duo,
✉ duoyq@chinasafety.ac.cn

RECEIVED 20 May 2024

ACCEPTED 18 June 2024

PUBLISHED 17 July 2024

CITATION

Zhang K, Chen S, Li Y, Duo Y and Wei L (2024),
Effects of equivalent ratio and initial
temperature on the explosion characteristics of
ethanol, acetone, and ethyl acetate.
Front. Energy Res. 12:1435466.
doi: 10.3389/fenrg.2024.1435466

COPYRIGHT

© 2024 Zhang, Chen, Li, Duo and Wei. This is an
open-access article distributed under the terms
of the [Creative Commons Attribution License
\(CC BY\)](https://creativecommons.org/licenses/by/4.0/). The use, distribution or reproduction in
other forums is permitted, provided the original
author(s) and the copyright owner(s) are
credited and that the original publication in this
journal is cited, in accordance with accepted
academic practice. No use, distribution or
reproduction is permitted which does not
comply with these terms.

Effects of equivalent ratio and initial temperature on the explosion characteristics of ethanol, acetone, and ethyl acetate

Kai Zhang¹, Sining Chen¹, Yanchao Li², Yingquan Duo^{1*} and Lijun Wei^{1*}

¹China Academy of Safety Science and Technology, Beijing, China, ²State Key Laboratory of Fine Chemicals, Department of Chemical Machinery and Safety Engineering, Dalian University of Technology, Dalian, China

In this paper, the effects of equivalence ratio (0.8–2.0) and temperature (30°C–120°C) on ethanol, acetone, and ethyl acetate vapors explosion characteristics through experimental and numerical studies were investigated. The explosion overpressure and flame propagation velocity were recorded through the pressure transducer and high-speed camera. The results showed that the flame propagation velocity, peak explosion overpressure, and peak growth rate of explosion overpressure increased first and then decreased with the increase of equivalence ratio. The cracks on the flame surface enhanced with the increase of the equivalence ratio. As the initial temperature increased, peak explosion overpressure, the flame propagation velocity, and peak growth rate of explosion overpressure gradually increased. The sensitivity analysis of laminar burning velocity indicated that with the change of equivalence ratio and initial temperature, the shared elementary reactions that increased the reactivity were $H + O_2 \rightleftharpoons O + OH$, $HCO + M \rightleftharpoons H + CO + M$, and $CO + OH \rightleftharpoons CO_2 + H$, and the shared elementary reaction that reduced the reactivity was $H + OH + M \rightleftharpoons H_2O + M$. The main factor affecting laminar burning velocity was the mole fraction of H and OH radicals.

KEYWORDS

vapor explosion, flame propagation velocity, explosion overpressure, laminar burning velocity, elementary reactions

1 Introduction

Ethanol, acetone, and ethyl acetate are common organic solvents for hazardous chemicals and are usually used in the chemical, petrochemical, pharmaceutical industries, and laboratories (Chow et al., 2021; Li Y. Q. et al., 2021; Nilaphai et al., 2022; Zhang et al., 2022). However, the inherent toxicity, corrosiveness, flammability, and explosiveness of these substances could bring great harm to human production and life. In recent years, due to the reduction of fossil fuels, these hazardous chemicals have been extensively investigated as potential alternative fuels (Zhang et al., 2018; Abdelkhalik et al., 2019; Oppong et al., 2020; Li X. L. et al., 2021; Mitu et al., 2021; Li et al., 2022). Since these substances are very easy to vaporize, once they leak into the air to form a combustible vapor mixture, there is a danger of vapor cloud explosion. Therefore, exploring the explosion

characteristics of ethanol, acetone, and ethyl acetate vapors with air is essential for the safe use of these hazardous chemicals.

The flame propagation and pressure characteristics of gases and dust have been extensively studied. Wu et al. (2021) used a Hartmann device and a spherical pressure vessel to test the ignition sensitivity and explosion severity of metal dust MH_2 ($M = Mg, Ti, Zr$), and the results showed that the reactivity and reaction rate of MgH_2 were higher than those of TiH_2 and ZrH_2 . The flame propagation velocity and structure, explosive residues, and combustion reaction mechanism of hydrogen/aluminum dust mixtures were elucidated by Yu et al. (2020). The results showed that the micro-diffusion flame and asymmetric flame appeared simultaneously in the flame propagation. Yang et al. (2021) conducted an explosion venting test of aluminum dust in a 20 L spherical chamber, and obtained the fitting formula of flame length and width, which provided a reference for the design of the venting safety area. Wang J. et al. (2020) explored the flame propagation characteristics of hydrogen/methane/air mixtures in pipes with different cross-sections. The results showed that the twists and folds of smooth flame front occurred when the flame propagates to mutation locations in the pipe cross-sectional area. The greater the mutation rate of the pipe, the more obvious the disturbance to the flame and the more serious the turbulence. Cao et al. (2021a), Cao et al. (2021b), Cao et al. (2021c), Cao et al. (2021d) conducted experimental and numerical simulation studies on the flame propagation and explosion pressure characteristics of hydrogen/air mixtures in spherical explosion containers and explosion venting devices. The influence laws of hydrogen concentration, opening pressure of explosion venting, and venting duct length on flame propagation and explosion pressure were obtained. The combined effects of the vertical concentration gradient and obstacle shape on the methane-air explosion characteristics were investigated experimentally by Huang et al. (2021). Li Y. C. et al. (2021) studied the correlation between the hydrogen/ammonia/air cloud explosion flame behavior and the maximum explosion pressure by changing the equivalence ratio. The results showed that the average flame propagation velocity and the maximum explosion pressure first increase and then decrease with the increase of the equivalence ratio.

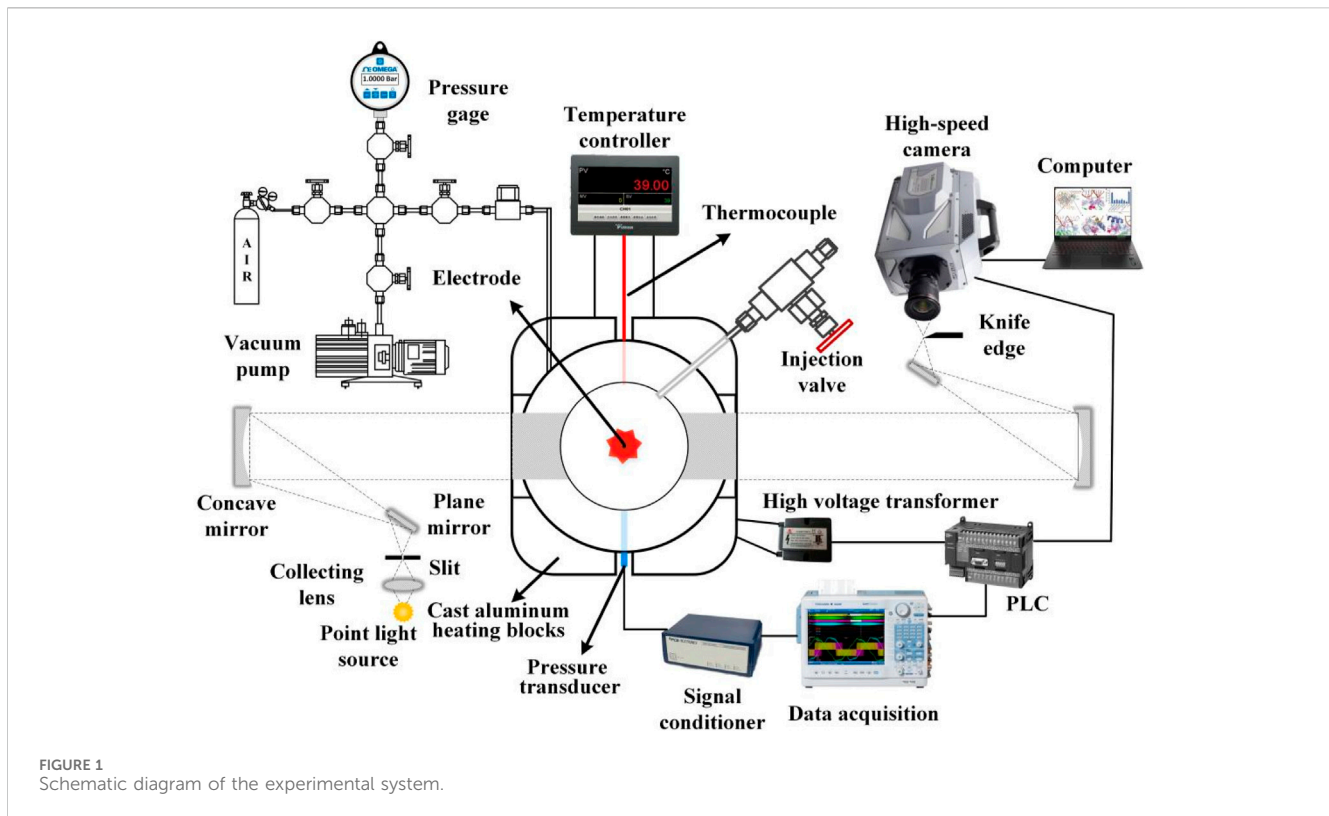
For the explosion characteristics of organic solvents, Song and Zhang (2021), Wang Z. R. et al. (2020), Cheng et al. (2021), and Mao et al. (2020) studied the flame propagation characteristics, flame temperature, pressure distribution, and thermal runaway of the organic solvent vapors, and deeply analyzed the reaction mechanism and pathway of the vapor cloud explosion. For the moment, some scholars have studied the explosion characteristics of ethanol, acetone, and ethyl acetate. Gerasimov et al. (2012), Saxena and Williams (2007), Sun et al. (2017), and Veloo et al. (2010), had investigated and improved the combustion mechanisms of ethanol through experimental and theoretical analysis. Mitu and Brandes (2017) researched the explosion characteristics of ethanol/air mixtures at various initial pressures (10.1–101 kPa), temperatures (298–373 K), and vessel volumes (5 L and 20 L). A linear relationship between the explosion pressure and the rate of pressure rise with the initial pressure was discovered. Bradley et al. (2009) measured the ethanol/air laminar burning velocity, the Markstein number, and the critical Peclet number at the beginning of flame instability under various initial pressures (0.1–1.4 MPa), temperatures (300–393 K),

and equivalence ratios. They discovered that the Markstein number decreased with the increase of the initial pressure, and slightly increased with the increase of temperature. Furthermore, several researchers (Beeckmann et al., 2014; Konnov et al., 2011; Mitu et al., 2018; Chen et al., 2021; Mol'Kov and Nekrasov, 1981) investigated the safety characteristics of ethanol/air mixtures under various initial pressure and temperature, and they obtained similar results. There are limited studies on the explosion characteristics of acetone/air mixtures. Chang et al. (2011) obtained the explosion overpressure and flammability limit region of acetone/air under various temperatures (150°C and 200°C) and pressure (101 and 202 kPa) using a 20 L standard spherical equipment and provided recommendations for the safe use of acetone. Chong and Hochgreb (2011), Mol'Kov and Nekrasov (1981), Nilsson et al. (2013), and Wu et al. (2016) evaluated the laminar burning velocity of acetone/air. The most critical elementary reactions impacting acetone/air laminar burning velocity are revealed to be $H + O_2 \rightleftharpoons O + OH$, $OH + CO \rightleftharpoons H + CO_2$, $HO_2 + CH_3 \rightleftharpoons OH + CH_3O$, $H + O_2 + H_2O \rightleftharpoons HO_2 + H_2O$. Dayma et al. (2012) observed laminar burning velocities of C_4 – C_7 Ethyl Esters (including ethyl acetate) in a 4.2 L spherical combustion chamber with various initial pressures (1–10 bar), temperatures (323–473 K), and equivalent ratios (0.7–1.5), and devised a novel combustion chemical reaction kinetic mechanism (1845 reactions versus 232 species). In the last 2 years, Li X. L. et al. (2021) and Oppong et al. (2021) have investigated the explosion characteristics of ethyl acetate/air mixtures and evaluated the explosion overpressure and laminar burning velocity under various initial pressures, temperatures, and equivalence ratios. They discovered that when the equivalence ratio and initial pressure increase, flame surface cracks and cell grids formed sooner, and the maximum explosion overpressure and laminar burning velocity approach an extreme value of 1.2. Badawy et al. (2016) measured the laminar burning velocity of ethyl propionate, ethyl butyrate, ethyl acetate, gasoline, and ethanol fuels under various equivalence ratios (0.8–1.4) and initial temperatures (60, 90, and 120°C). The flame propagation velocity, Markstein length, Markstein number, laminar burning velocity, and laminar burning flux were calculated and analyzed. The results showed that the unstretched flame propagation velocity of ethanol was the fastest, and that of ethyl acetate was the slowest. The highest unstretched flame velocity was in the equivalence ratio range of $\Phi = 1.1$ – 1.2 .

This work aimed to investigate the explosion characteristics of ethanol, acetone, and ethyl acetate vapors at various equivalent ratios and initial temperatures through experimental and numerical studies. The flame development patterns of three liquid vapors were compared. The results of experimental and numerical studies of flame propagation velocity, peak explosion overpressure, and peak growth rate of explosion overpressure were analyzed. The potential explosion overpressure of three liquid vapors was estimated. Finally, the effects of elementary reactions and active radicals on the laminar combustion rate were investigated.

2 Materials and methods

Figure 1 shows the schematic diagram of the experimental system, including a spherical vessel (100 mm inner diameter),



high-speed schlieren system, ignition system, heating system, synchronous control system, and gas distribution and liquid injection system. A FASTCAM SA-Z high-speed camera was used to capture the flame propagation behavior through a schlieren system and quartz glasses (25 mm in diameter) with a capture rate of 10,000 fps. A PCB (Model: 113B24) pressure transducer was used to collect the pressure data with an acquisition frequency of 100 kS/s. The heating system can provide a uniform and stable initial temperature for the spherical vessel after heating for 2 h. A 15 kV high-voltage transformer was adopted as an ignition source, which can generate approximately 10 W of energy. The breaking current was 30 mA, and the discharge duration was 0.3 s. A pair of tungsten rods of 1 mm diameter with the electrode tips spacing of 1 mm was employed as the electrode. Some other detailed parameters can be found in Zhang et al. (2022).

The experiment was carried out according to the following steps: 1) heating the spherical vessel to the required temperature, 2) vacuuming the vessel, 3) injecting the required liquid into the vessel through a pipette and preparing the corresponding air, 4) activating the timing controller, 5) recording the pressure and flame propagation data. An OMEGA pressure gauge with a range of 0–689.48 kPa and an accuracy of 0.05% was used to prepare the gas by the partial pressure method. Assuming that the liquid was completely transformed into an ideal gas in a vacuum environment, the volume fraction of the liquid vapor was calculated as Eq. 1:

$$\varphi = \frac{L \cdot d \cdot (T + 273)}{M \cdot p_0} \cdot \frac{V_0 \cdot p_s}{V \cdot (T_0 + 273)} \cdot 100\% \quad (1)$$

The equivalence ratio was defined as Eq. 2:

$$\Phi = \frac{n_{fuel}/n_{air}}{(n_{fuel}/n_{air})_{st}} \quad (2)$$

In this study, ethanol, acetone, and ethyl acetate were purchased from Tianjin Kemiou Chemical Reagent Co., Ltd., and the purity is 99.5%. The compressed air was purchased from Dalian Junfeng Gas Chemical Co., Ltd., and the composition was 21% oxygen and 79% nitrogen. The information of the three substances is listed in Table 1.

Figure 2 illustrates the typical curves of explosion overpressure with changing equivalence ratio and initial temperature. In the initial stage of flame propagation, the variation of explosion overpressure was negligible. When the vapor was burnt, the explosion overpressure started to rise rapidly and reached the peak value. When the vapor was burnt out, the explosion overpressure decreased subsequently. For the ethanol explosion at a given initial temperature and initial pressure (60°C, 100 kPa), both peak explosion overpressure and growth rate of explosion overpressure increased until $\Phi = 1.4$, then decreased with the increase of equivalence ratio. For ethanol explosion at a given equivalence ratio and initial pressure ($\Phi = 1$, 100 kPa), the peak explosion overpressure gradually decreased with the increase of initial temperature. The peak explosion overpressure and growth rate of explosion overpressure are directly affected by the variation of experimental parameters and are used to characterize the explosion intensity of liquid vapor clouds.

The explosion overpressure and laminar burning velocity of ethanol, acetone, and ethyl acetate at various equivalent ratios and temperatures were calculated using the premixed laminar flame velocity calculation module in ANSYS CHEMKIN PRO, and the

TABLE 1 The physical properties of ethanol, acetone, and ethyl acetate.

Substance	Ethanol	Acetone	Ethyl acetate (EA)
Molecular formula	C ₂ H ₆ O	C ₃ H ₆ O	C ₄ H ₈ O ₂
Molecule schematic	$\begin{array}{c} \text{H} \quad \text{H} \\ \quad \\ \text{H}-\text{C}-\text{C}-\text{OH} \\ \quad \\ \text{H} \quad \text{H} \end{array}$	$\begin{array}{c} \text{H} \quad \text{O} \quad \text{H} \\ \quad \quad \\ \text{H}-\text{C}-\text{C}-\text{C}-\text{H} \\ \quad \\ \text{H} \quad \text{H} \end{array}$	$\begin{array}{c} \text{H} \quad \text{O} \quad \text{H} \quad \text{H} \\ \quad \quad \quad \\ \text{H}-\text{C}-\text{C}-\text{O}-\text{C}-\text{C}-\text{H} \\ \quad \quad \quad \\ \text{H} \quad \text{H} \quad \text{H} \quad \text{H} \end{array}$
Molecular mass	46.07	58.08	88.10
Flammability limit (%)	3.3–19	2.2–13	2–11.5
Melting point (°C)	-114	-94.9	-83.6
Boiling point (°C)	78.3	56.53	77.2
Flash point (°C)	12	-20	-4
Density (20°C, g/cm ³)	0.794	0.790	0.897
Heat of combustion (kJ/mol)	-1365.5	-1788.7	-2247.89

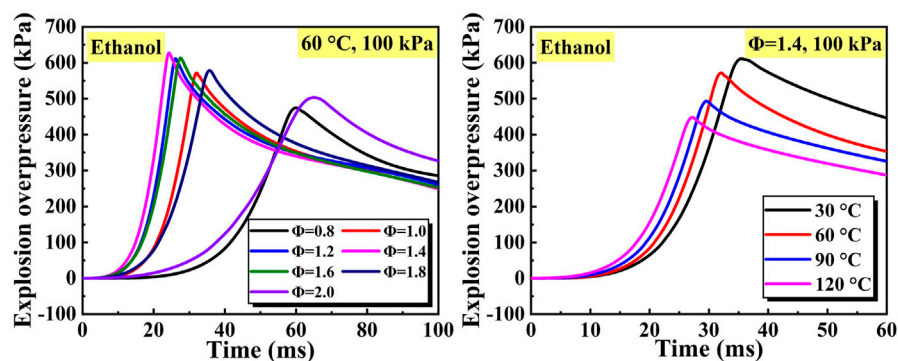


FIGURE 2 Typical curves of explosion overpressure changing equivalence ratio and initial temperature.

sensitivity of the elementary reaction to the laminar burning velocity was evaluated. Besides, GASEQ was used to calculate the density of the unburned and burned mixture. The mechanism reported by Sun et al. (2017) was used in the numerical calculation. To obtain accurate calculation results, the maximum number of grid points was set to 3000, the solution gradient and curvature were set to 0.01, and the ending axial point was set to 1 cm.

3 Results and discussions

3.1 Effects of equivalence ratio

Figures 3–5 illustrate the effects of equivalence ratio on flame behavior of C₂H₆O, C₃H₆O, and C₄H₈O₂ liquid vapor explosions. With the change from the lean side to the rich side, the propagating flame of different liquid vapor explosions tended to be more unstable. Specifically, several cracks appeared on the rich flame surface and the cracks will grow with time. The appearance and growth of cracks are caused by flame instabilities (Gárzon Lama

et al., 2021; Oppong et al., 2021; Li et al., 2022; Zuo et al., 2022), when the flame radius exceeds a critical value, the cracks will even be generated by cellular structures. Therefore, C₂H₆O, C₃H₆O, and C₄H₈O₂ liquid vapor explosions on the rich side were more susceptible to flame instabilities. In addition, the flame arrival time of different liquid vapor explosions, in which the propagating flame reached a fixed scale, firstly decreased and then increased with the increase of equivalence ratio.

Figure 6 shows the effects of equivalence ratio on flame propagation velocity (FPV) of different liquid vapor explosions. The experimental FPV was calculated based on the relationship between flame radius and flame arrival time in the visualization window. The numerical FPV was calculated by Eq. 3, ignoring the stretch effects (Burke et al., 2009; Ai et al., 2014; Song et al., 2020):

$$V_N = \rho_u / \rho_b \cdot S_L \quad (3)$$

As shown in Figure 6, the FPV of experimental and numerical firstly increased and then decreased with the increase of equivalence ratio. The equivalence ratios corresponding to the peak value of experimental FPV of C₂H₆O, C₃H₆O, and C₄H₈O₂ liquid vapor

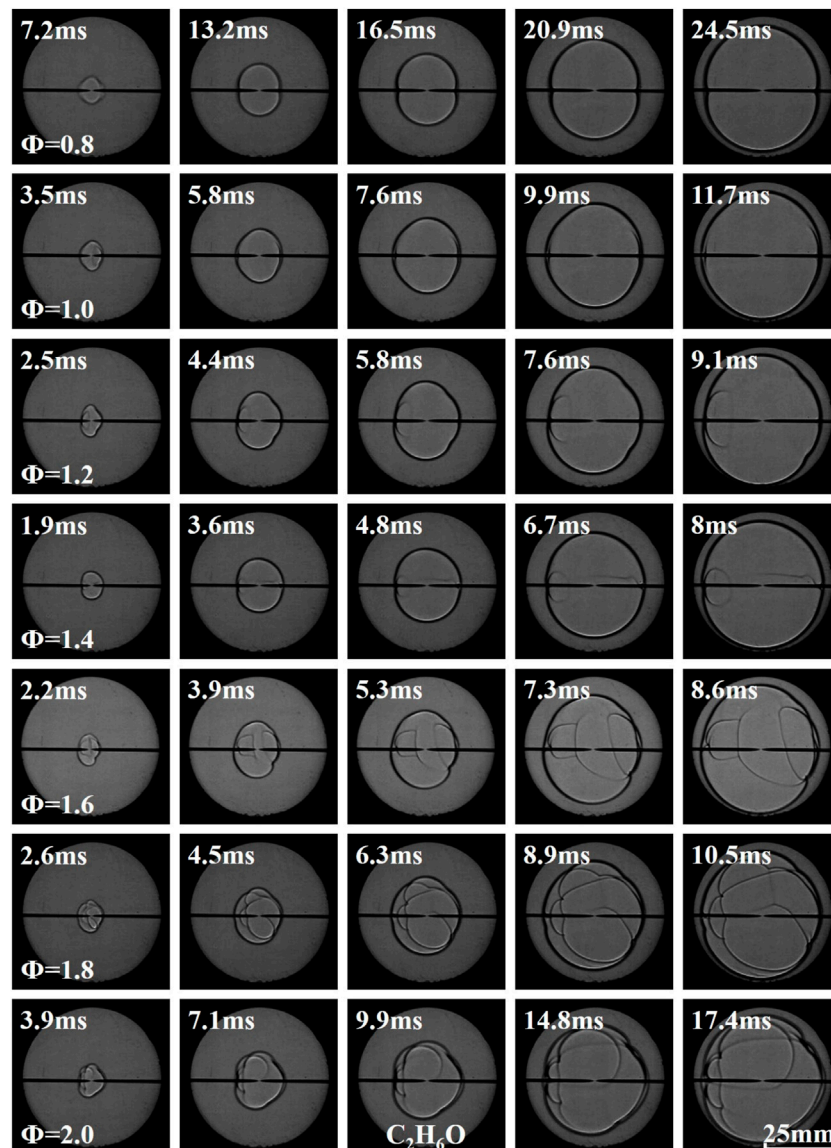


FIGURE 3 Effects of equivalence ratio on flame behavior of C_2H_6O liquid vapor explosion.

explosions were $\Phi = 1.4$, $\Phi = 1.4$, and $\Phi = 1.2$, respectively. The equivalence ratios corresponding to the peak value of numerical FPV of C_2H_6O , C_3H_6O , and $C_4H_8O_2$ liquid vapor explosions were all $\Phi = 1.2$.

Figure 7 expresses the effects of equivalence ratio on peak explosion overpressure (PEO) of different liquid vapor explosions. The numerical PEO was calculated using the CHEMKIN. Obviously, with the increase of equivalence ratio, the PEO of experimental and numerical of different liquid vapor explosions firstly increased and then decreased. And the peak values of experimental and numerical PEO were reached at $\Phi = 1.2$ and $\Phi = 1.4$. In addition, the values of numerical PEO of different liquid vapor explosions were higher than experimental PEO, which could be attributed to the heat loss (Li et al., 2018). The adiabatic conditions were set in the numerical simulations, but it was difficult to be maintained due to heat conduction, heat convection, and heat radiation.

Figure 8 shows the effects of equivalence ratio on the peak growth rate of explosion overpressure (PGREO) of different liquid vapor explosions. The PGREO of different liquid vapor explosions firstly increased and then decreased with the increase of equivalence ratio. The equivalence ratios corresponding to the peak value of PGREO of C_2H_6O , C_3H_6O , and $C_4H_8O_2$ vapor explosions were $\Phi = 1.4$, $\Phi = 1.2$, and $\Phi = 1.4$, respectively. For a given equivalence ratio, the PGREO of C_2H_6O vapor explosions were slightly higher than that of C_3H_6O and $C_4H_8O_2$ vapor explosions.

3.2 Effects of initial temperature

Figures 9–11 present the effects of initial temperature on flame behavior of C_2H_6O , C_3H_6O , and $C_4H_8O_2$ liquid vapor explosions. With the increase of initial temperature, the propagating flame of

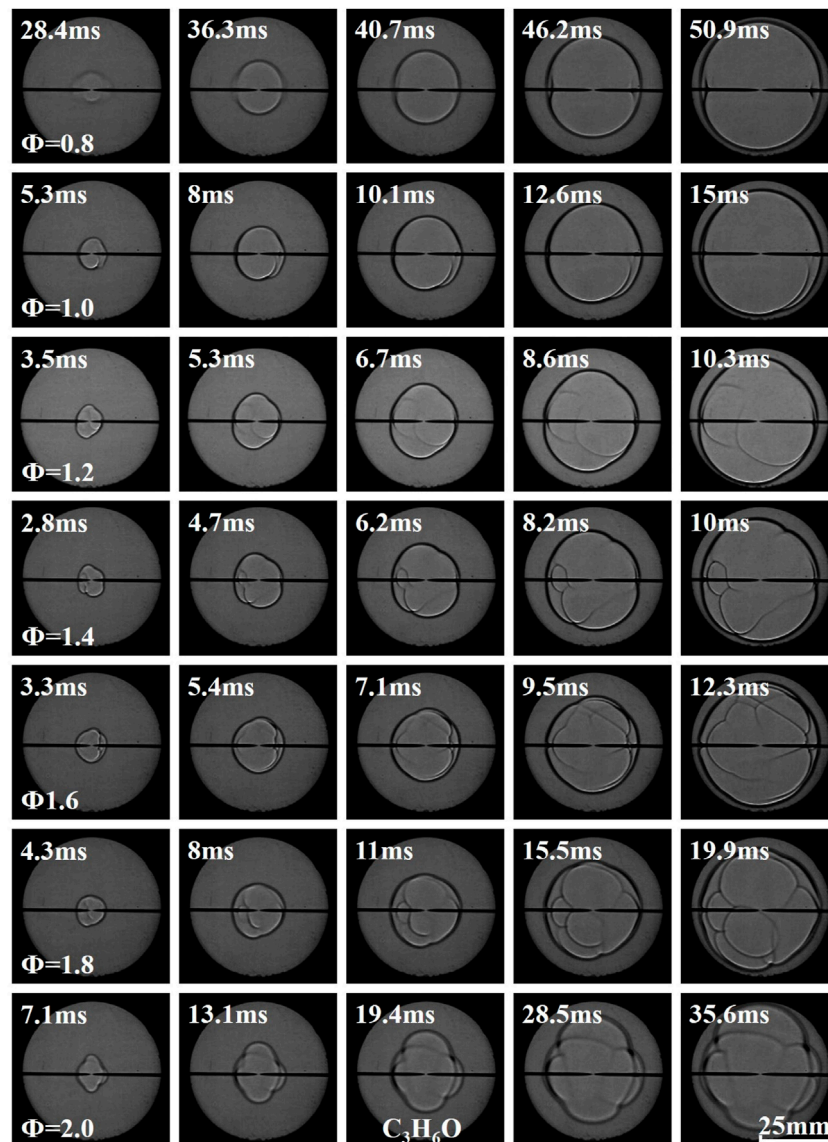


FIGURE 4 Effects of equivalence ratio on flame behavior of C_3H_6O liquid vapor explosion.

different liquid vapor explosions was relatively smooth, which indicated that the flame instabilities were almost unchanged by increasing initial temperature. In addition, the flame arrival time of different liquid vapor explosions decreased with the increase of initial temperature.

In Figure 12, the effects of initial temperature on flame propagation velocity (FPV) of different liquid vapor explosions are shown. With the increase of initial temperature, the FPV of different liquid vapor explosions in experimental and numerical continued to increase. However, the numerical FPV of different liquid vapor explosions was higher than the experimental value.

Figure 13 shows the effects of initial temperature on peak explosion overpressure (PEO) of different liquid vapor explosions. As the initial temperature changes from $30^\circ C$ to $120^\circ C$, the PEO of different liquid vapor explosions in experimental and numerical continued to decrease. And at

different initial temperatures, the numerical PEO of different liquid vapor explosions was higher than the experimental value due to the heat loss.

The Effects of initial temperature on the peak growth rate of explosion overpressure (PGREO) of different liquid vapor explosions are shown in Figure 14. With the increase of initial temperature, the PGREO of different liquid vapor explosions continued to increase. For a given initial temperature, the increasing order of PGREO was $C_4H_8O_2$, C_3H_6O , and C_2H_6O .

Generally, with the increase of equivalence ratio, all of FPV, PEO, and PGREO of different liquid vapor explosions firstly increased and then decreased. This is mainly due to the fact that with the increase of equivalent ratio, the fuel goes through the process of poor combustion to rich combustion. However, FPV, PEO, and PGREO are relatively small in both poor and rich combustion, so they increase first and then decrease. With the

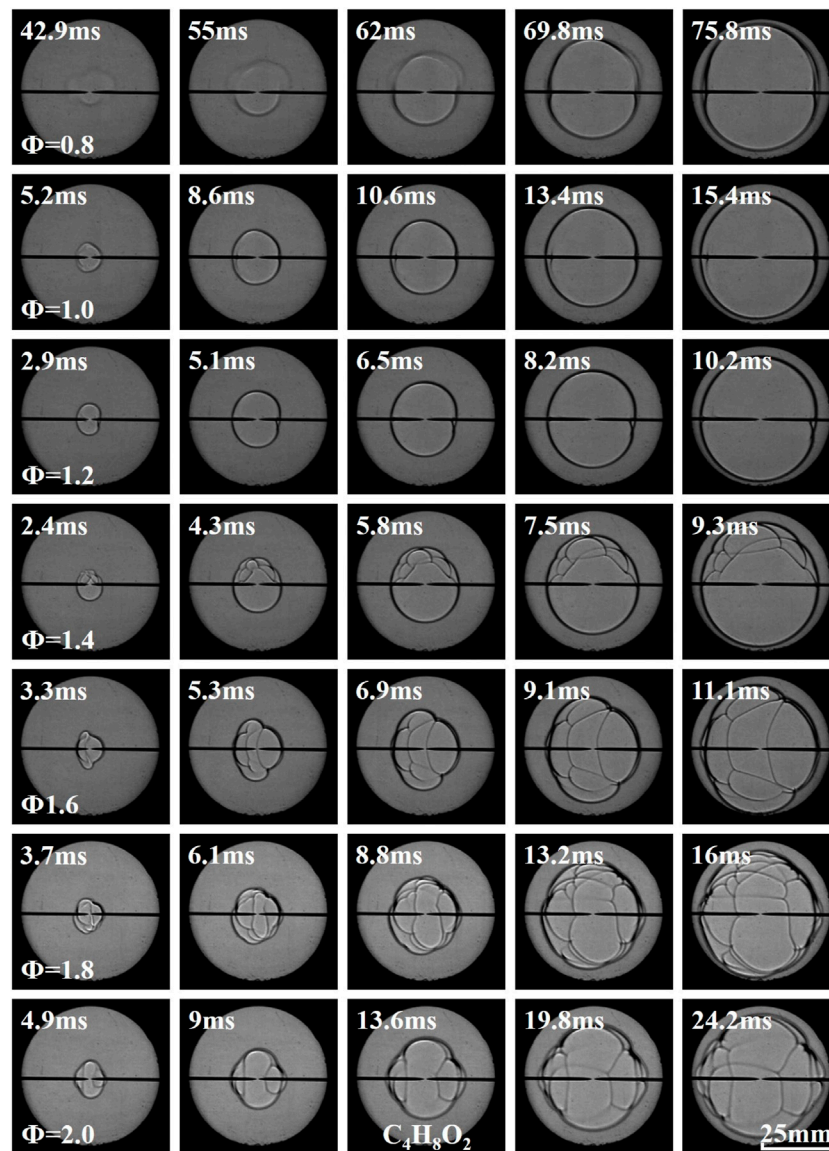


FIGURE 5 Effects of equivalence ratio on flame behavior of $C_4H_8O_2$ liquid vapor explosion.

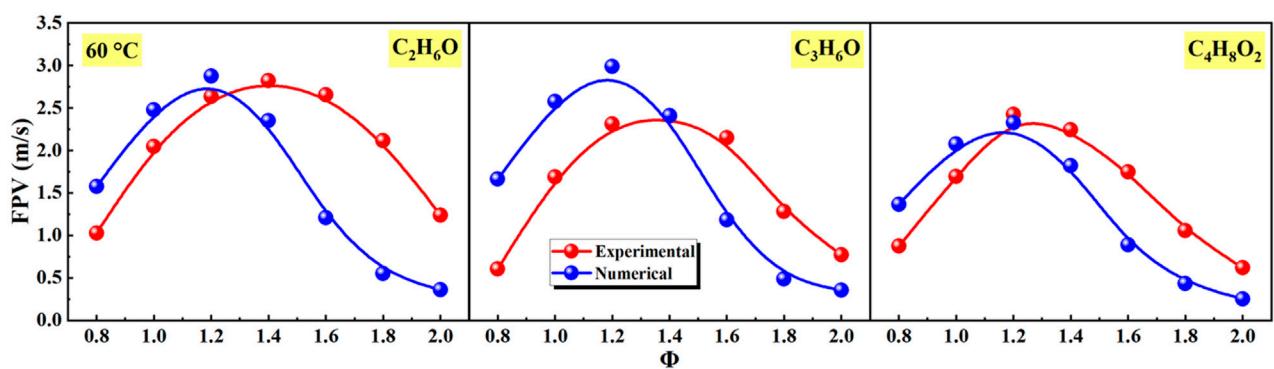


FIGURE 6 Effects of equivalence ratio on flame propagation velocity (FPV) of different liquid vapor explosions.

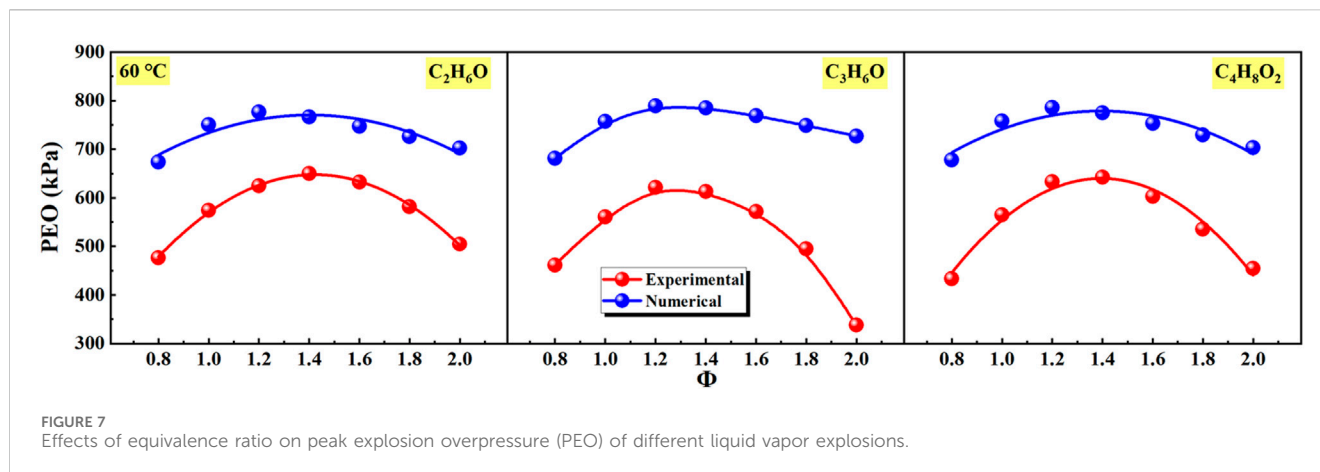


FIGURE 7 Effects of equivalence ratio on peak explosion overpressure (PEO) of different liquid vapor explosions.

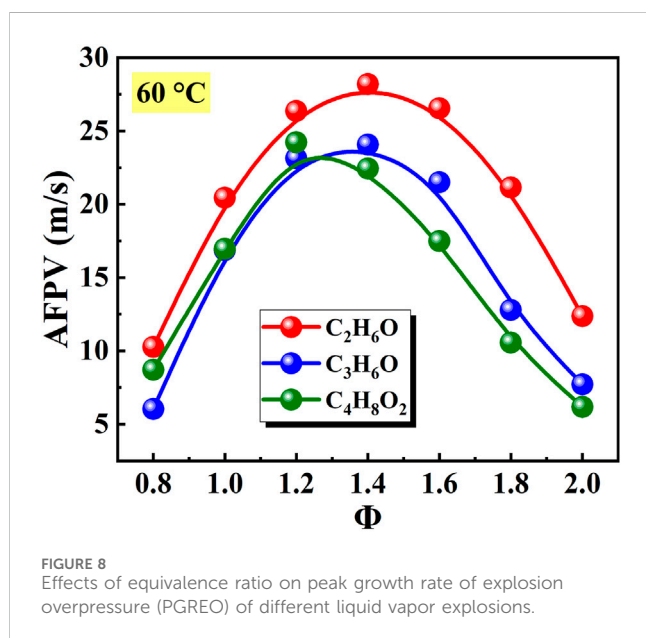


FIGURE 8 Effects of equivalence ratio on peak growth rate of explosion overpressure (PGREO) of different liquid vapor explosions.

increase of initial temperature, the PEO of different liquid vapor explosions continued to decrease, the FPV and PGREO gradually increased. This is mainly due to the fact that the increase in temperature speeds up the molecular motion rate and greatly increases the collision frequency between molecules. Therefore, the reaction is more intense, and both FPV and PGREO increase. In the constant volume explosion, the maximum explosion pressure is inversely proportional to the initial temperature, so the PEO decreases with the increase of initial temperature.

3.3 Kinetic factors affecting laminar burning velocity

As shown in Figure 6 and Figure 12, with the increase of equivalence ratio and initial temperature, the FPV of different liquid vapor explosions was highly related to laminar burning velocity. To reveal the relationship of laminar burning velocity and explosion overpressure, the explosion overpressure of

different liquid vapor explosions was calculated using Eq. 4 (Bradley and Mitcheson, 1976; Dahoe et al., 1996):

$$\frac{dp}{dt} = \frac{3(p_e - p_0)}{R} \cdot \left(\frac{p}{p_0}\right)^{\frac{1}{n}} \cdot \left[1 - \left(\frac{p_0}{p}\right)^{\frac{1}{n}} \cdot \frac{p_e - p}{p_e - p_0}\right]^{\frac{3}{2}} \cdot S \quad (4)$$

Figure 15 shows the explosion overpressure of different liquid vapor explosions by theoretical calculation. The calculated explosion overpressure was almost unchanged in the initial stage, then increased rapidly with time. The variation tendency of theoretical and experimental explosion overpressure was consistent. However, differences in the quantitative characteristics were existent. The reasons were that the constant laminar burning velocity was assumed and the flame instabilities were ignored in Eq. 4.

Both FPV and explosion overpressure of different liquid vapor explosions were closely depended on laminar burning velocity. In view of this, the laminar burning velocity of different liquid vapor explosions was discussed in this subsection and the factors affecting laminar burning velocity were explored from the perspective of reaction kinetics.

Figure 16 shows the effects of equivalence ratio and initial temperature on the laminar burning velocity of different liquid vapor explosions. As the equivalence ratio increased from $\Phi = 0.8$ to $\Phi = 2.0$, the laminar burning velocity of different vapor explosions firstly increased and then decreased. The equivalence ratios corresponding to the peak value of the laminar burning velocity of C_2H_6O , C_3H_6O , and $C_4H_8O_2$ vapor explosions were $\Phi = 1.2$, $\Phi = 1.2$, and $\Phi = 1.0$. For a given equivalence ratio, the decreasing order of laminar burning velocity was C_2H_6O , C_3H_6O , and $C_4H_8O_2$. In addition, as the initial temperature increased from $30^\circ C$ to $120^\circ C$, the laminar burning velocity of different liquid vapor explosions continuously increased. For a given initial temperature, the decreasing order of laminar burning velocity was C_2H_6O , C_3H_6O , and $C_4H_8O_2$.

For the C_3H_6O explosion, as the equivalence ratio changed, the elementary reactions that enhancing reaction activity were: $H + O_2 \rightleftharpoons O + OH$, $CO + OH \rightleftharpoons CO_2 + H$, $HCO + M \rightleftharpoons H + CO + M$, $HCCO + O_2 \rightleftharpoons CO_2 + CO + H$. The elementary reactions that reducing reaction activity were: $CH_3 + H (+M) \rightleftharpoons CH_4 (+M)$, $CH_3COCH_3 + H \rightleftharpoons CH_3COCH_2 + H_2$, $HCO + H \rightleftharpoons CO + H_2$, $H + OH + M \rightleftharpoons H_2O + M$.

For the $C_4H_8O_2$, as the equivalence ratio changed, the elementary reactions that enhancing reaction activity were: $H + O_2 \rightleftharpoons O + OH$,

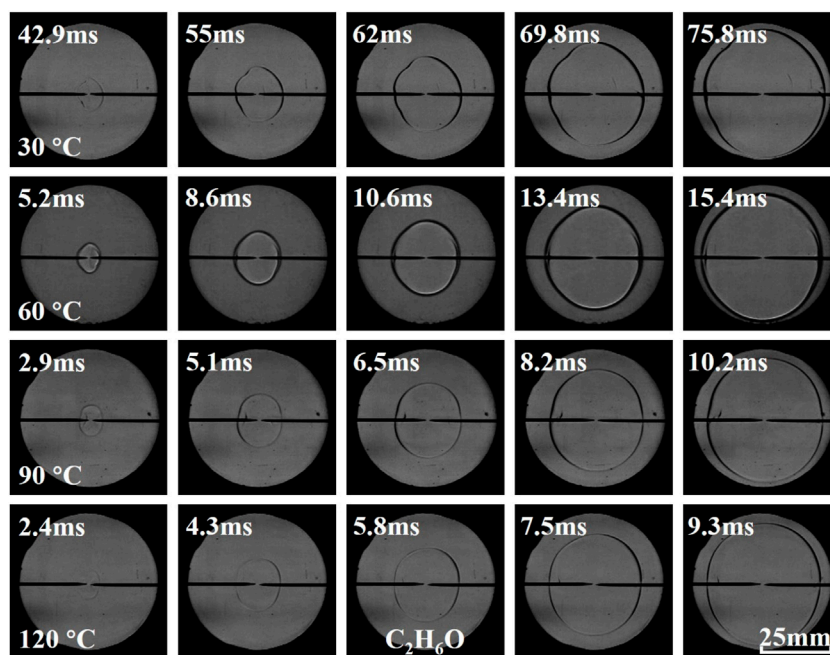


FIGURE 9
Effects of initial temperature on flame behavior of C_2H_6O liquid vapor explosion.

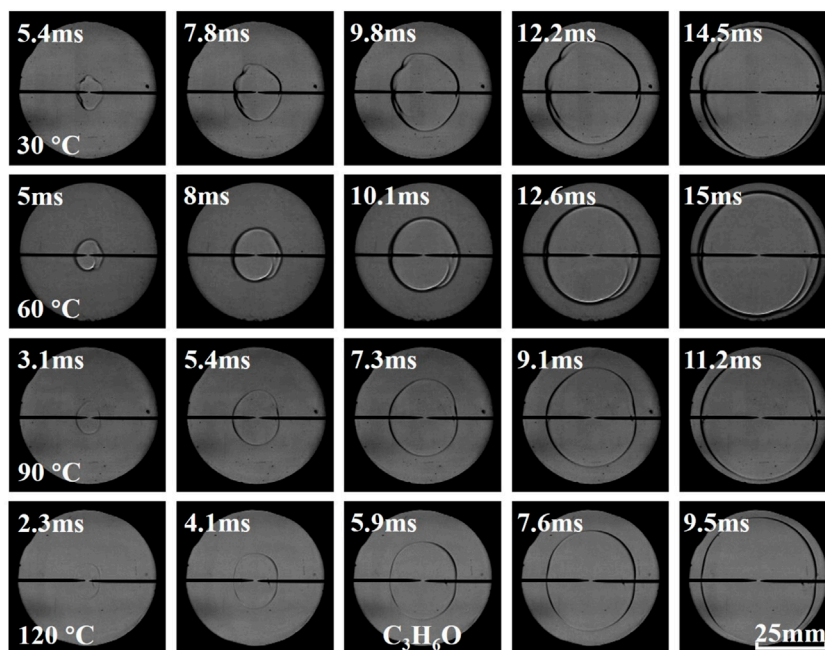


FIGURE 10
Effects of initial temperature on flame behavior of C_3H_6O liquid vapor explosion.

$HCO + M \rightleftharpoons H + CO + M$, $CO + OH \rightleftharpoons CO_2 + H$, $EA \rightleftharpoons C_2H_4 + CH_3COOH$. The elementary reactions that reducing reaction activity were: $CH_3 + H (+M) \rightleftharpoons CH_4 (+M)$, $C_2H_3 + H \rightleftharpoons C_2H_2 + H_2$, $CH_2CO + H \rightleftharpoons CH_3 + CO$, $H + OH + M \rightleftharpoons H_2O + M$.

Totally, for different liquid vapor explosions, the shared elementary reactions that enhancing reaction activity under different equivalence ratios were: $H + O_2 \rightleftharpoons O + OH$, $HCO + M \rightleftharpoons H + CO + M$, $CO + OH \rightleftharpoons CO_2 + H$. The shared

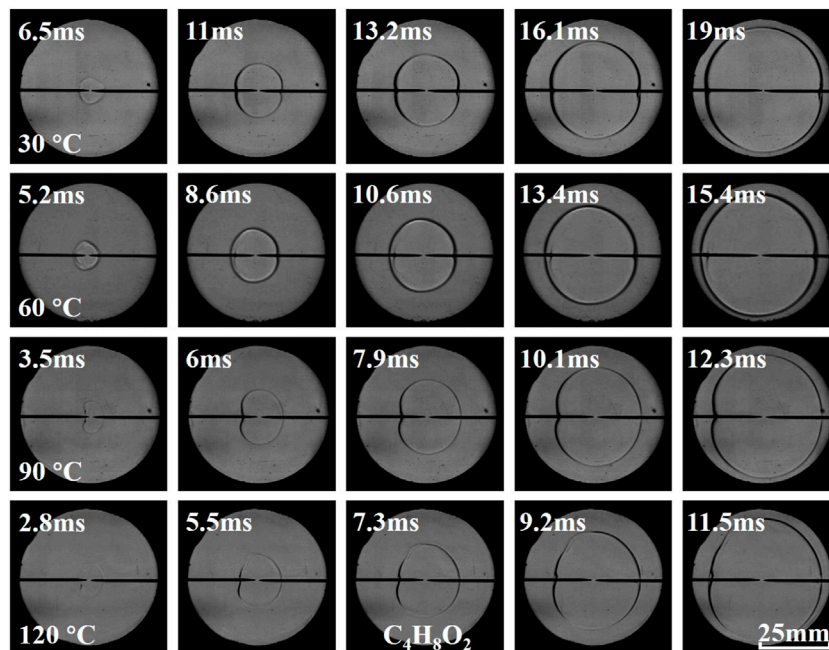


FIGURE 11 Effects of initial temperature on flame behavior of $C_4H_8O_2$ liquid vapor explosion.

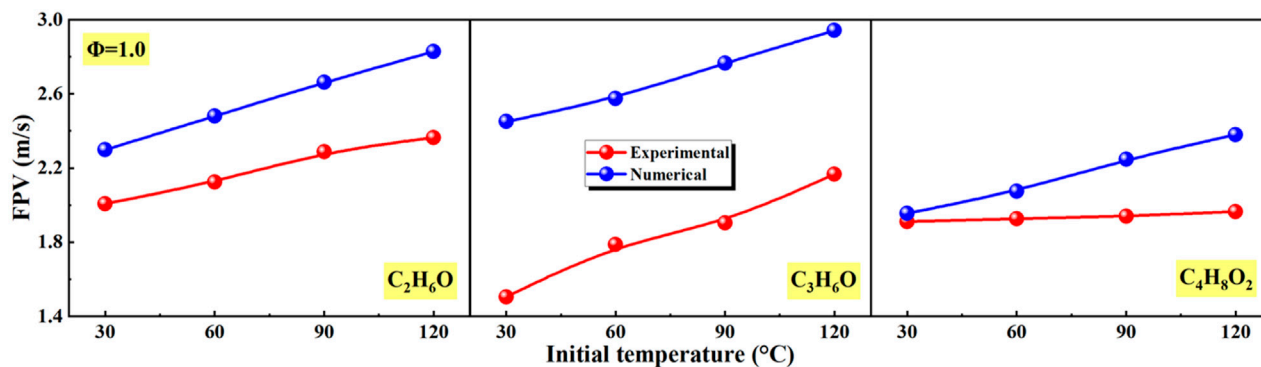


FIGURE 12 Effects of initial temperature on flame propagation velocity (FPV) of different liquid vapor explosions.

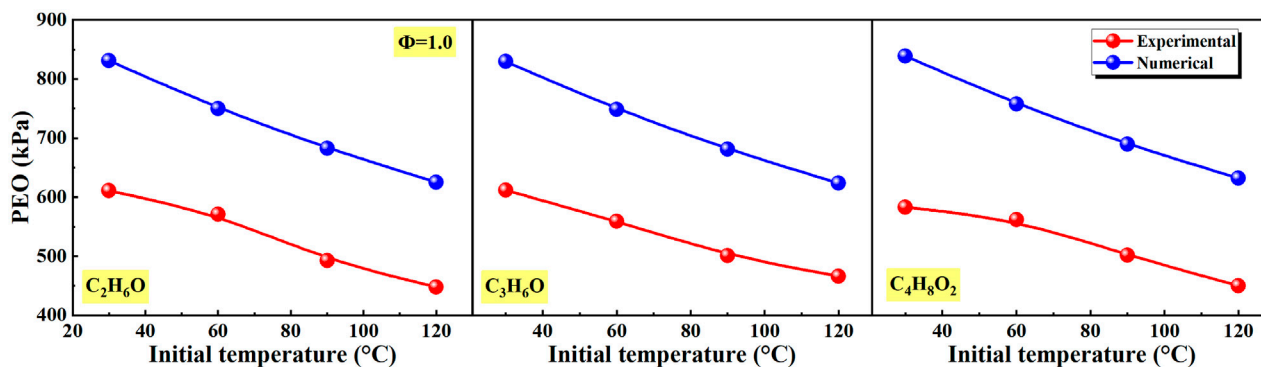
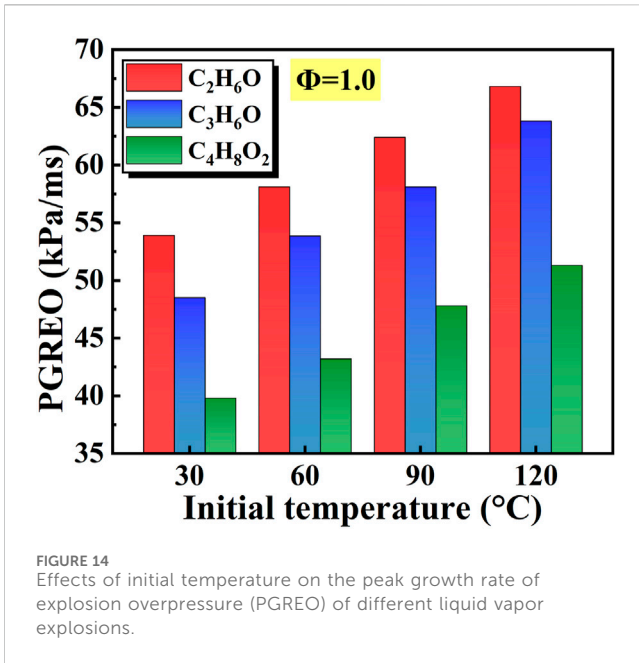


FIGURE 13 Effects of initial temperature on peak explosion overpressure (PEO) of different liquid vapor explosions.

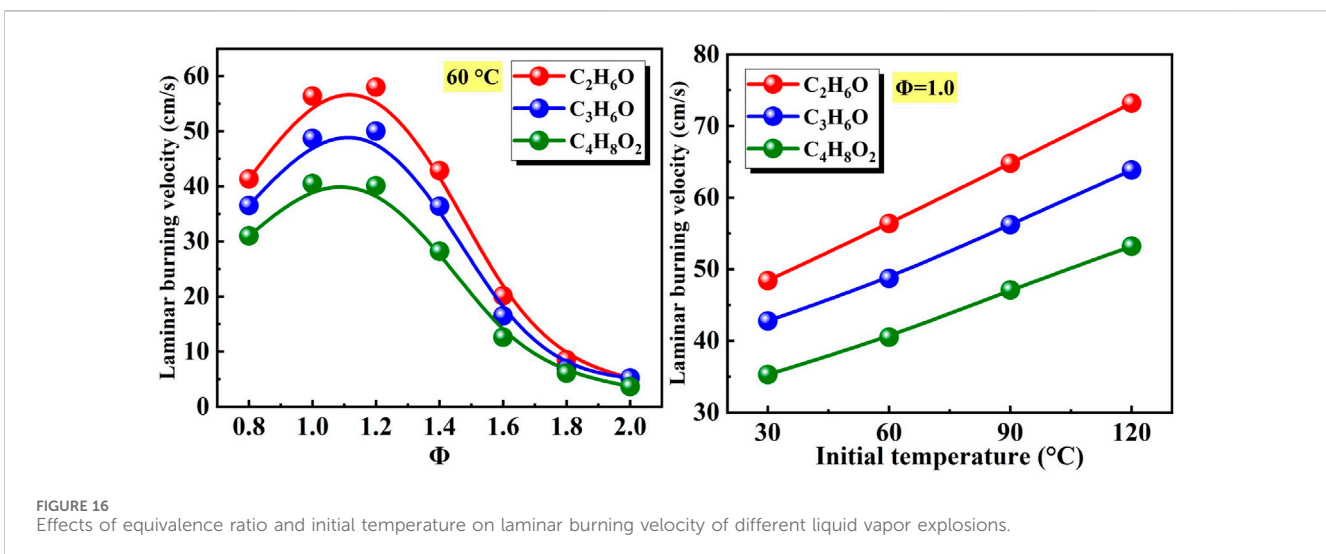
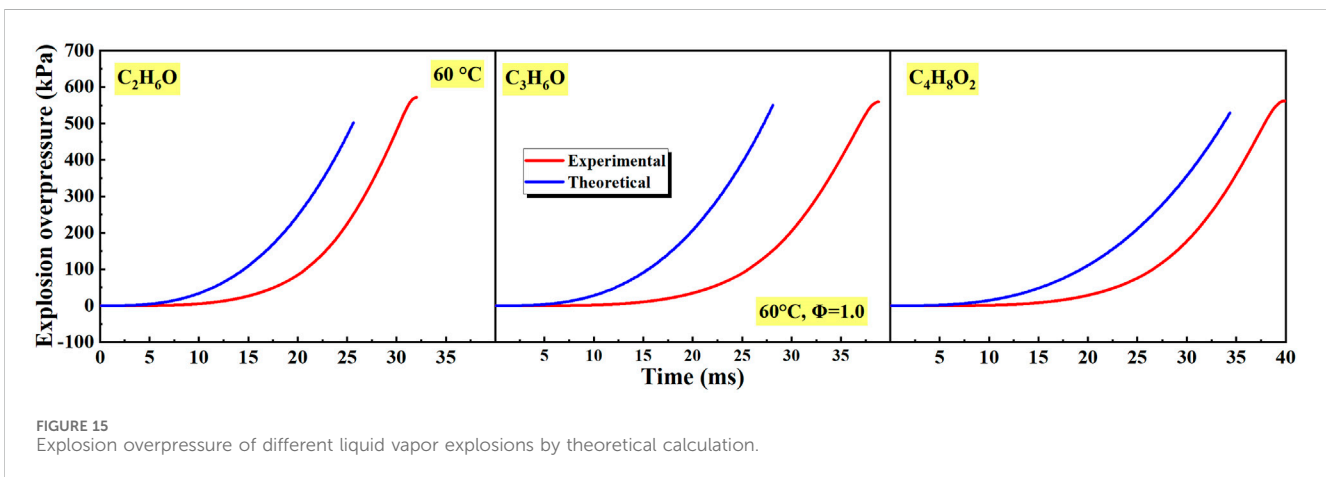


elementary reactions that reducing reaction activity were: $\text{CH}_3 + \text{H} (+\text{M}) \rightleftharpoons \text{CH}_4 (+\text{M})$, $\text{H} + \text{OH} + \text{M} \rightleftharpoons \text{H}_2\text{O} + \text{M}$.

For the $\text{C}_3\text{H}_6\text{O}$ explosion, as the initial temperature changed, the elementary reactions that enhancing reaction activity were: $\text{H} + \text{O}_2 \rightleftharpoons \text{O} + \text{OH}$, $\text{CO} + \text{OH} \rightleftharpoons \text{CO}_2 + \text{H}$, $\text{HCO} + \text{M} \rightleftharpoons \text{H} + \text{CO} + \text{M}$, $\text{HCCO} + \text{O}_2 \rightleftharpoons \text{CO}_2 + \text{CO} + \text{H}$. The elementary reactions that reducing reaction activity were: $\text{CH}_3 + \text{H} (+\text{M}) \rightleftharpoons \text{CH}_4 (+\text{M})$, $\text{HCO} + \text{H} \rightleftharpoons \text{CO} + \text{H}_2$, $\text{H} + \text{O}_2 (+\text{M}) \rightleftharpoons \text{HO}_2 (+\text{M})$, $\text{H} + \text{OH} + \text{M} \rightleftharpoons \text{H}_2\text{O} + \text{M}$.

For the $\text{C}_4\text{H}_8\text{O}_2$ explosion, as the initial temperature changed, the elementary reactions that enhancing reaction activity were: $\text{H} + \text{O}_2 \rightleftharpoons \text{O} + \text{OH}$, $\text{CO} + \text{OH} \rightleftharpoons \text{CO}_2 + \text{H}$, $\text{HCO} + \text{M} \rightleftharpoons \text{H} + \text{CO} + \text{M}$, $\text{EA} \rightleftharpoons \text{C}_2\text{H}_4 + \text{CH}_3\text{COOH}$. The elementary reactions that reducing reaction activity were: $\text{H} + \text{OH} + \text{M} \rightleftharpoons \text{H}_2\text{O} + \text{M}$, $\text{H} + \text{O}_2 (+\text{M}) \rightleftharpoons \text{HO}_2 (+\text{M})$, $\text{HCO} + \text{H} \rightleftharpoons \text{CO} + \text{H}_2$, $\text{HCO} + \text{OH} \rightleftharpoons \text{CO} + \text{H}_2\text{O}$.

Totally, for different liquid vapor explosions, the shared elementary reactions that enhancing reaction activity under different initial temperatures were: $\text{H} + \text{O}_2 \rightleftharpoons \text{O} + \text{OH}$, $\text{CO} + \text{OH} \rightleftharpoons \text{CO}_2 + \text{H}$, $\text{HCO} + \text{M} \rightleftharpoons \text{H} + \text{CO} + \text{M}$. The shared elementary reactions that reducing reaction activity were: $\text{H} + \text{O}_2 (+\text{M}) \rightleftharpoons \text{HO}_2 (+\text{M})$, $\text{H} + \text{OH} + \text{M} \rightleftharpoons \text{H}_2\text{O} + \text{M}$, $\text{HCO} + \text{H} \rightleftharpoons \text{CO} + \text{H}_2$.



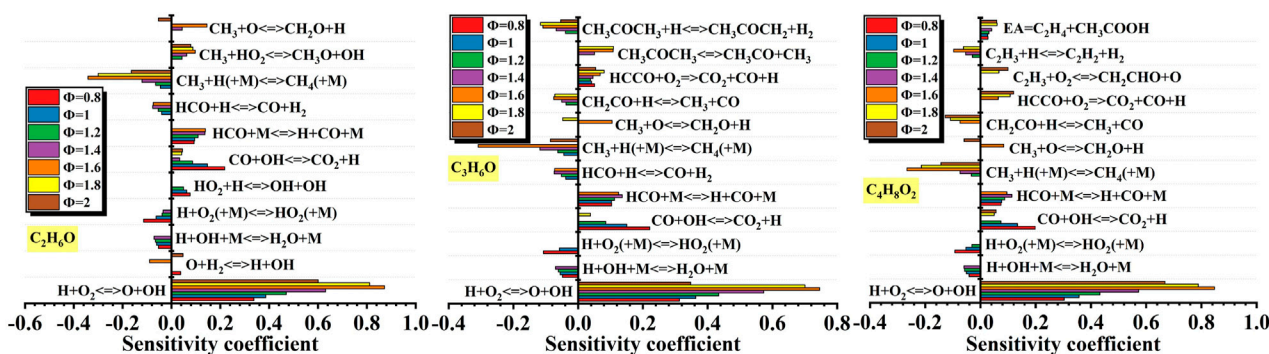


FIGURE 17 Effects of equivalence ratio on sensitivity coefficient of different liquid vapor explosions. Figure 17 shows the effects of equivalence ratio on sensitivity coefficient of different liquid vapor explosions. For the C₂H₆O, as the equivalence ratio changed, the elementary reactions that enhancing reaction activity were: H + O₂ <=> O + OH, CO + OH <=> CO₂ + H, HCO + M <=> H + CO + M and CH₃ + HO₂ <=> CH₃O + OH. The elementary reactions that reducing reaction activity were: CH₃ + H (+M) <=> CH₄ (+M), HCO + H <=> CO + H₂, H + O₂ (+M) <=> HO₂ (+M), H + OH + M <=> H₂O + M.

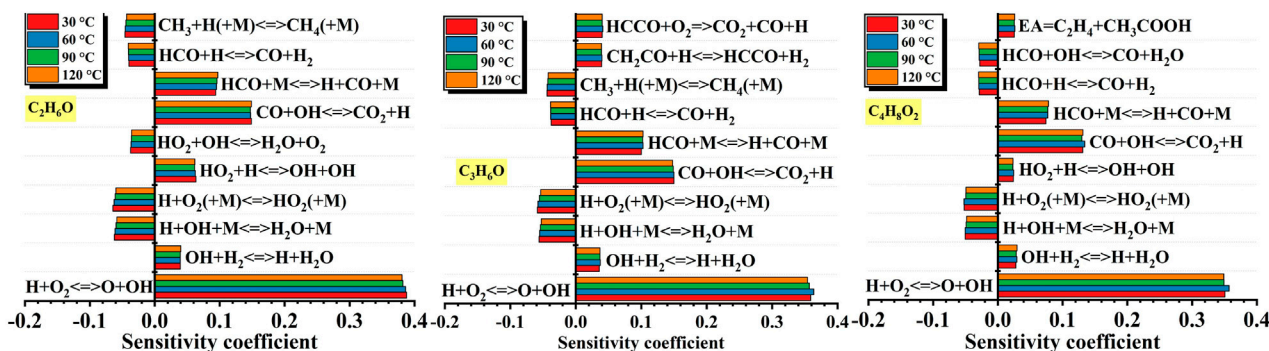


FIGURE 18 Effects of initial temperature on sensitivity coefficient of different liquid vapor explosions. Figure 18 shows the effects of initial temperature on sensitivity coefficient of different liquid vapor explosions. For the C₂H₆O explosion, as the initial temperature changed, the elementary reactions that enhancing reaction activity were: H + O₂ <=> O + OH, CO + OH <=> CO₂ + H, HCO + M <=> H + CO + M, HO₂ + H <=> OH + OH. The elementary reactions that reducing reaction activity were: CH₃ + H (+M) <=> CH₄ (+M), HCO + H <=> CO + H₂, H + O₂ (+M) <=> HO₂ (+M), H + OH + M <=> H₂O + M.

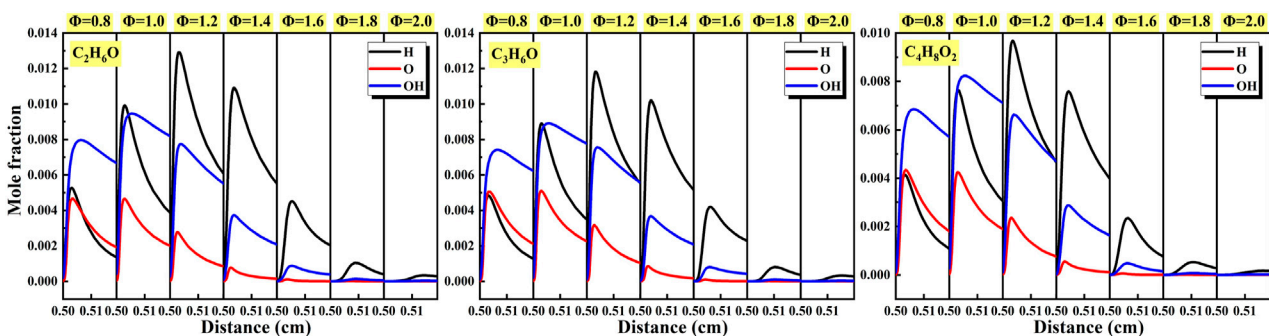
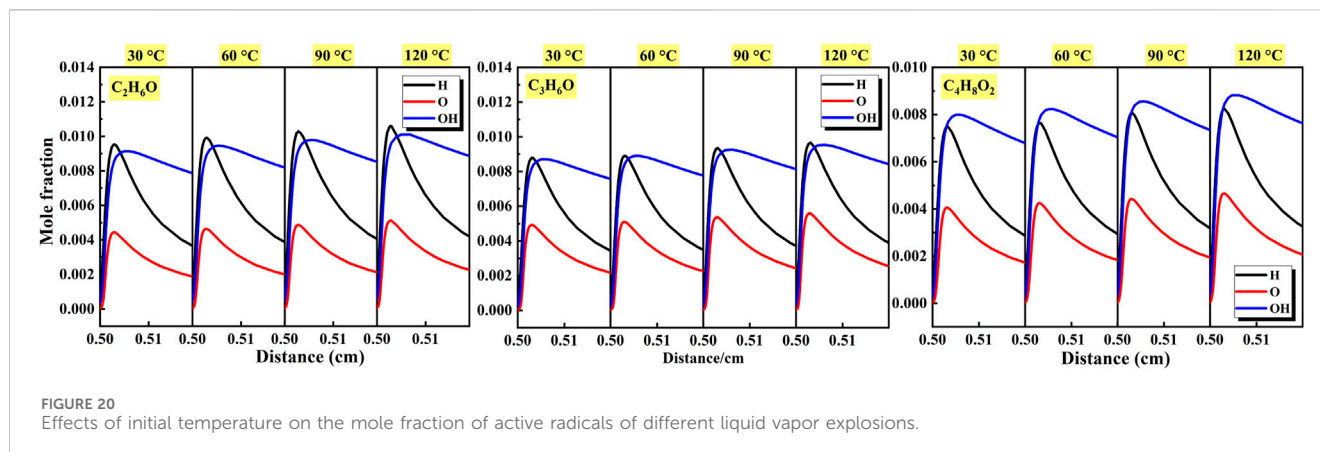


FIGURE 19 Effects of equivalence ratio on the mole fraction of active radicals of different liquid vapor explosions.

As shown in Figure 19 and Figure 20, the generation and consumption of active radicals in the important elementary reactions affecting reaction activity are displayed and the characteristics of active radicals of different liquid vapor

explosions were analyzed. Figure 19 shows the effects of equivalence ratio on the mole fraction of active radicals of different liquid vapor explosions. For different liquid vapor explosions, the maximum mole fraction of H radical increased



until $\Phi = 1.2$ and then decreased with the increase of equivalence ratio. The tendency was highly consistent with the maximum mole fraction of OH radical, and its peak value was reached when $\Phi = 1.0$. In addition, the maximum mole fraction of O radical at $\Phi = 0.8$ and $\Phi = 1.0$ was almost the same, then gradually decreased with the increase of equivalence ratio. Figure 20 shows the effects of initial temperature on the mole fraction of active radicals of different liquid vapor explosions. With the increase of initial temperature, the maximum mole fraction of active radicals of different liquid vapor explosions gradually increased.

4 Conclusion

This paper obtained a general understanding of the effects of equivalence ratios (0.8–2.0) and temperatures (30°C–120°C) on ethanol, acetone, and ethyl acetate vapors explosion characteristics through experimental and numerical studies. The explosion overpressure and flame propagation were recorded through a pressure transducer and high-speed camera. The relationship between laminar burning velocity and explosion overpressure was also revealed. The conclusions are as follows.

- (1) The flame propagation velocity, peak explosion overpressure, and peak growth rate of explosion overpressure of ethanol, acetone, and ethyl acetate vapors showed a trend of first increasing and then decreasing with the increase of equivalence ratio, and they almost all reached the peak when $\Phi = 1.2$ or $\Phi = 1.4$. The cracks on the flame surface increased with the increase of the equivalence ratio.
- (2) With the increase of the initial temperature, peak explosion overpressure of ethanol, acetone, and ethyl acetate vapor explosions continued to decrease, and the flame propagation velocity and peak growth rate of explosion overpressure gradually increased. Maintaining the same temperature, the increasing order of peak growth rate of explosion overpressure was ethyl acetate, acetone, and ethanol.

- (3) The laminar burning velocity and explosion overpressure had a tight connection. From the perspective of chemical reaction kinetics, the elementary reactions affecting the laminar burning velocity were discussed. For the three liquid vapors, with the change of equivalent ratio, the shared elementary reactions enhancing the reactivity were $\text{H} + \text{O}_2 \rightleftharpoons \text{O} + \text{OH}$, $\text{HCO} + \text{M} \rightleftharpoons \text{H} + \text{CO} + \text{M}$, and $\text{CO} + \text{OH} \rightleftharpoons \text{CO}_2 + \text{H}$. The shared elementary reactions reducing the reactivity were $\text{CH}_3 + \text{H} (+\text{M}) \rightleftharpoons \text{CH}_4 (+\text{M})$ and $\text{H} + \text{OH} + \text{M} \rightleftharpoons \text{H}_2\text{O} + \text{M}$. With the change of the initial temperature, the shared elementary reactions increasing the reactivity were $\text{H} + \text{O}_2 \rightleftharpoons \text{O} + \text{OH}$, $\text{CO} + \text{OH} \rightleftharpoons \text{CO}_2 + \text{H}$, and $\text{HCO} + \text{M} \rightleftharpoons \text{H} + \text{CO} + \text{M}$. The shared elementary reactions reducing the reactivity were $\text{H} + \text{O}_2 (+\text{M}) \rightleftharpoons \text{HO}_2 (+\text{M})$, $\text{H} + \text{OH} + \text{M} \rightleftharpoons \text{H}_2\text{O} + \text{M}$, and $\text{HCO} + \text{H} \rightleftharpoons \text{CO} + \text{H}_2$.
- (4) For the three liquid vapor explosions, the maximum mole fraction of H radical continued to increase until $\Phi = 1.2$, and then decreased as the equivalence ratio increased. This trend was highly consistent with the maximum mole fraction of OH radical, and its peak value reached $\Phi = 1.0$. In addition, when $\Phi = 0.8$ and $\Phi = 1.0$, the maximum mole fraction of O radical was almost the same, and then gradually decreased as the equivalence ratio increased. With the increase of the initial temperature, the maximum mole fraction of reactive radicals of different liquid vapor explosions gradually increased.

Data availability statement

The original contributions presented in the study are included in the article/Supplementary Material, further inquiries can be directed to the corresponding authors.

Author contributions

KZ: Data curation, Investigation, Methodology, Resources, Writing—original draft, Writing—review and editing. SC: Investigation, Methodology, Writing—original draft, Writing—review and editing, Resources. YL: Investigation,

Methodology, Resources, Writing—original draft, Writing—review and editing, Data curation, Software. YD: Investigation, Methodology, Resources, Writing—original draft, Writing—review and editing, Data curation, Funding acquisition. LW: Investigation, Methodology, Writing—original draft, Writing—review and editing.

Funding

The author(s) declare that financial support was received for the research, authorship, and/or publication of this article. The authors appreciate the financial support by the National Key R&D Program of China (No. 2023YFC3008801).

References

- Abdelkhalik, A., Askar, E., Markus, D., Brandes, E., and Stolz, T. (2019). Explosion regions of acetone and alcohol/inert gas/air mixtures at high temperatures and atmospheric pressure. *J. Loss Prev. Proc.* 62, 103958. doi:10.1016/j.jlp.2019.103958
- Ai, Y. H., Zhou, Z., Chen, Z., and Kong, W. J. (2014). Laminar flame speed and Markstein length of syngas at normal and elevated pressures and temperatures. *Fuel* 137, 339–345. doi:10.1016/j.fuel.2014.08.004
- Badawy, T., Williamson, J., and Xu, H. M. (2016). Laminar burning characteristics of ethyl propionate, ethyl butyrate, ethyl acetate, gasoline and ethanol fuels. *Fuel* 183, 627–640. doi:10.1016/j.fuel.2016.06.087
- Beekmann, J., Cai, L., and Pitsch, H. (2014). Experimental investigation of the laminar burning velocities of methanol, ethanol, n-propanol, and n-butanol at high pressure. *Fuel* 117 (A), 340–350. doi:10.1016/j.fuel.2013.09.025
- Bradley, D., Lawes, M., and Mansour, M. S. (2009). Explosion bomb measurements of ethanol-air laminar flame characteristics at pressures up to 1.4MPa. *Combust. Flame* 156 (7), 1462–1470. doi:10.1016/j.combustflame.2009.02.007
- Bradley, D., and Mitcheson, A. (1976). Mathematical solutions for explosions in spherical vessels. *Combust. Flame* 26, 201–217. doi:10.1016/0010-2180(76)90072-9
- Burke, M. P., Chen, Z., Ju, Y. G., and Dryer, F. L. (2009). Effect of cylindrical confinement on the determination of laminar flame speeds using outwardly propagating flames. *Combust. Flame* 156 (4), 771–779. doi:10.1016/j.combustflame.2009.01.013
- Cao, W. G., Li, W. J., Yu, S., Zhang, Y., Shu, C. M., Liu, Y. F., et al. (2021a). Explosion venting hazards of temperature effects and pressure characteristics for premixed hydrogen-air mixtures in a spherical container. *Fuel* 290, 120034. doi:10.1016/j.fuel.2020.120034
- Cao, W. G., Li, W. J., Zhang, L., Chen, J. F., Yu, S., Zhou, Z. H., et al. (2021b). Flame characteristics of premixed H₂-air mixtures explosion venting in a spherical container through a duct. *Int. J. Hydrogen Energy* 46 (52), 26693–26707. doi:10.1016/j.ijhydene.2021.05.148
- Cao, W. G., Li, W. J., Zhang, Y., Zhou, Z. H., Zhao, Y. M., Yang, Z. X., et al. (2021c). Experimental study on the explosion behaviors of premixed syngas-air mixtures in ducts. *Int. J. Hydrogen Energy* 46 (44), 23053–23066. doi:10.1016/j.ijhydene.2021.04.120
- Cao, W. G., Zhou, Z. H., Li, W. J., Zhao, Y. M., Yang, Z. X., Zhang, Y., et al. (2021d). Under-expansion jet flame propagation characteristics of premixed H₂/air in explosion venting. *Int. J. Hydrogen Energy* 46 (78), 38913–38922. doi:10.1016/j.ijhydene.2021.09.109
- Chang, Y. M., You, M. L., Lin, C. H., Wu, S. Y., Tseng, J. M., Lin, C. P., et al. (2011). Fire and explosion hazard evaluation for the acetone aqueous solutions. *J. Therm. Anal. Calorim.* 106 (1), 179–189. doi:10.1007/s10973-011-1605-7
- Chen, J., Zhao, Y. L., Bi, Y. B., Li, C. H., Kong, D. P., and Lu, S. X. (2021). Effect of initial pressure on the burning behavior of ethanol pool fire in the closed pressure vessel. *Process Saf. Environ.* 153, 159–166. doi:10.1016/j.psep.2021.07.022
- Cheng, Z., Ni, L., Wang, J. J., Jiang, J. C., Yao, H., Chen, Q., et al. (2021). Process hazard evaluation and exothermic mechanism for the synthesis of n-butylmagnesium bromide Grignard reagent in different solvents. *Process Saf. Environ.* 147, 654–673. doi:10.1016/j.psep.2020.12.041
- Chong, C. T., and Hochgreb, S. (2011). Measurements of laminar flame speeds of acetone/methane/air mixtures. *Combust. Flame* 158 (3), 490–500. doi:10.1016/j.combustflame.2010.09.019
- Chow, M. R., Ooi, J. B., Chee, K. M., Pun, C. H., Tran, M. V., Leong, J. C. K., et al. (2021). Effects of ethanol on the evaporation and burning characteristics of palm-oil based biodiesel droplet. *J. Energy Inst.* 98, 35–43. doi:10.1016/j.joei.2021.05.008

Conflict of interest

The authors declare that the research was conducted in the absence of any commercial or financial relationships that could be construed as a potential conflict of interest.

Publisher's note

All claims expressed in this article are solely those of the authors and do not necessarily represent those of their affiliated organizations, or those of the publisher, the editors and the reviewers. Any product that may be evaluated in this article, or claim that may be made by its manufacturer, is not guaranteed or endorsed by the publisher.

Dahoe, A. E., Zevenbergen, J. F., Lemkowitz, S. M., and Scarlett, B. (1996). Dust explosions in spherical vessels: the role of flame thickness in the validity of the cube-root law. *J. Loss Prev. Proc.* 9 (1), 33–44. doi:10.1016/0950-4230(95)00054-2

Dayma, G., Halter, F., Foucher, F., Mounaim-Rousselle, C., and Dagaut, P. (2012). Laminar burning velocities of C4-C7 ethyl esters in a spherical combustion chamber: experimental and detailed kinetic modeling. *Energ. Fuel* 26 (11), 6669–6677. doi:10.1021/ef301254q

Gárzon Lama, L. F. M., Pizzuti, L., Sotton, J., and Martins, C. A. (2021). Experimental investigation of hydrous ethanol/air flame front instabilities at elevated temperature and pressures. *Fuel* 287, 119555. doi:10.1016/j.fuel.2020.119555

Gerasimov, I. E., Knyazkov, D. A., Yakimov, S. A., Bolshova, T. A., Shmakov, A. G., and Korobeinichev, O. P. (2012). Structure of atmospheric-pressure fuel-rich premixed ethylene flame with and without ethanol. *Combust. Flame* 159 (5), 1840–1850. doi:10.1016/j.combustflame.2011.12.022

Huang, C. Y., Chen, X. F., Liu, L. Y., Zhang, H. M., Yuan, B. H., and Li, Y. (2021). The influence of opening shape of obstacles on explosion characteristics of premixed methane-air with concentration gradients. *Process Saf. Environ.* 150, 305–313. doi:10.1016/j.psep.2021.04.028

Konnov, A. A., Meuwissen, R. J., and de Goey, L. P. H. (2011). The temperature dependence of the laminar burning velocity of ethanol flames. *P. Combust. Inst.* 33 (1), 1011–1019. doi:10.1016/j.proci.2010.06.143

Li, X. L., Wang, Q. W., Oppong, F., Liu, W. N., and Xu, C. S. (2021a). Cellularization characteristics of ethyl acetate spherical expanding flame. *Fuel* 291, 120213. doi:10.1016/j.fuel.2021.120213

Li, Y., Xu, W., Jiang, Y., and Liew, K. M. (2022). Effects of diluents on laminar burning velocity and cellular instability of 2-methyltetrahydrofuran-air flames. *Fuel* 308, 121974. doi:10.1016/j.fuel.2021.121974

Li, Y. C., Bi, M. S., Li, B., Zhou, Y. H., and Gao, W. (2018). Effects of hydrogen and initial pressure on flame characteristics and explosion pressure of methane/hydrogen fuels. *Fuel* 233, 269–282. doi:10.1016/j.fuel.2018.06.042

Li, Y. C., Bi, M. S., Zhou, Y. H., Zhang, Z. L., Zhang, K., Zhang, C. S., et al. (2021b). Characteristics of hydrogen-ammonia-air cloud explosion. *Process Saf. Environ.* 148, 1207–1216. doi:10.1016/j.psep.2021.02.037

Li, Y. Q., Cao, Z., Chen, Y., and Wu, G. (2021c). A synthetic skeletal mechanism for combustion simulation of acetone-n-butanol-ethanol mixture and its components in diesel engines. *Fuel* 290, 120097. doi:10.1016/j.fuel.2020.120097

Mao, B. B., Chen, H. D., Jiang, L., Zhao, C. P., Sun, J. H., and Wang, Q. S. (2020). Refined study on lithium ion battery combustion in open space and a combustion chamber. *Process Saf. Environ.* 139, 133–146. doi:10.1016/j.psep.2020.03.037

Mitu, M., and Brandes, E. (2017). Influence of pressure, temperature and vessel volume on explosion characteristics of ethanol/air mixtures in closed spherical vessels. *Fuel* 203, 460–468. doi:10.1016/j.fuel.2017.04.124

Mitu, M., Brandes, E., and Hirsch, W. (2018). Mitigation effects on the explosion safety characteristic data of ethanol/air mixtures in closed vessel. *Process Saf. Environ.* 117, 190–199. doi:10.1016/j.psep.2018.04.024

Mitu, M., Stolz, T., Brandes, E., and Zakel, S. (2021). Burning and explosion behaviour of ethanol/water-sucrose mixtures. *J. Loss Prev. Proc.* 71, 104451. doi:10.1016/j.jlp.2021.104451

Mol'Kov, V. V., and Nekrasov, V. P. (1981). Normal propagation velocity of acetone-air flames versus pressure and temperature. *Combust. Explos. Shock* 17 (3), 280–283. doi:10.1007/BF00751300

- Nilaphai, O., Komancey, K., and Chuepeng, S. (2022). Expansion heat release and thermal efficiency of acetone-butanol-ethanol-diesel blended fuel (ABE20) combustion in piston engine. *Fuel* 309, 122214. doi:10.1016/j.fuel.2021.122214
- Nilsson, E. J. K., de Goey, L. P. H., and Konnov, A. A. (2013). Laminar burning velocities of acetone in air at room and elevated temperatures. *Fuel* 105, 496–502. doi:10.1016/j.fuel.2012.07.047
- Oppong, F., Luo, Z. Y., Li, X. L., and Xu, C. S. (2021). Investigations on explosion characteristics of ethyl acetate. *J. Loss Prev. Proc.* 70, 104409. doi:10.1016/j.jlp.2021.104409
- Oppong, F., Xu, C. S., Luo, Z. Y., Li, X. L., Zhou, W. H., Wu, S. Y., et al. (2020). Investigating the explosion of ethyl acetate in the presence of hydrogen. *Int. J. Hydrogen Energy* 45 (39), 20400–20407. doi:10.1016/j.ijhydene.2019.12.136
- Saxena, P., and Williams, F. A. (2007). Numerical and experimental studies of ethanol flames. *P. Combust. Inst.* 3 (1), 1149–1156. doi:10.1016/j.proci.2006.08.097
- Song, J. H., Cho, S. H., Lee, K. M., and Park, J. (2020). Measurements of laminar burning velocity and Markstein length in outwardly-propagating spherical SNG-air premixed flames at elevated pressures. *Fuel* 275, 117952. doi:10.1016/j.fuel.2020.117952
- Song, Y. F., and Zhang, Q. (2021). Explosion effect of vapor-liquid two-phase n-heptane at various initial temperatures. *Process Saf. Environ.* 145, 303–311. doi:10.1016/j.psep.2020.08.021
- Sun, W. Y., Tao, T., Zhang, R. Z., Liao, H. D., Huang, C., Zhang, F., et al. (2017). Experimental and modeling efforts towards a better understanding of the high-temperature combustion kinetics of C3-C5 ethyl esters. *Combust. Flame* 185, 173–187. doi:10.1016/j.combustflame.2017.07.013
- Veloo, P. S., Wang, Y. L., Egofoopoulos, F. N., and Westbrook, C. K. (2010). A comparative experimental and computational study of methanol, ethanol, and n-butanol flames. *Combust. Flame* 157 (10), 1989–2004. doi:10.1016/j.combustflame.2010.04.001
- Wang, J., Wu, Y., Zheng, L. G., Yu, M. G., Pan, R. K., and Shan, W. W. (2020a). Study on the propagation characteristics of hydrogen/methane/air premixed flames in variable cross-section ducts. *Process Saf. Environ.* 135, 135–143. doi:10.1016/j.psep.2019.12.029
- Wang, Z. R., Jiao, F., Cao, X. Y., Jiang, K. W., Ma, S. C., and Yin, Z. L. (2020b). Mechanisms of vapor cloud explosion and its chain reaction induced by an explosion venting flame. *Process Saf. Environ.* 141, 18–27. doi:10.1016/j.psep.2020.05.018
- Wu, X. L., Xu, S., Pang, A. M., Cao, W. G., Liu, D. B., Zhu, X. Y., et al. (2021). Hazard evaluation of ignition sensitivity and explosion severity for three typical MH2 (M= Mg, Ti, Zr) of energetic materials. *Def. Technol.* 17 (4), 1262–1268. doi:10.1016/j.dt.2020.06.011
- Wu, Y., Modica, V., Rossow, B., and Grisch, F. (2016). Effects of pressure and preheating temperature on the laminar flame speed of methane/air and acetone/air mixtures. *Fuel* 185, 577–588. doi:10.1016/j.fuel.2016.07.110
- Yang, M. R., Jiang, H. P., Chen, X. F., and Gao, W. (2021). Characteristic evaluation of aluminum dust explosion venting with high static activation pressure. *Process Saf. Environ.* 152, 83–96. doi:10.1016/j.psep.2021.05.039
- Yu, X. Z., Yu, J. L., Zhang, X. Y., Ji, W. T., Lv, X. S., Hou, Y. J., et al. (2020). Combustion behaviors and residues characteristics in hydrogen/aluminum dust hybrid explosions. *Process Saf. Environ.* 134, 343–352. doi:10.1016/j.psep.2019.12.023
- Zhang, K., Gao, W., Li, Y. C., Zhang, Z. L., Shang, S., Zhang, C. S., et al. (2022). Lower flammability limits of ethanol, acetone and ethyl acetate vapor mixtures in air. *J. Loss Prev. Proc.* 74, 104676. doi:10.1016/j.jlp.2021.104676
- Zhang, S. F., Lee, T. H., Wu, H., Pei, J. Y., Wu, W., Liu, F. S., et al. (2018). Experimental and kinetic studies on laminar flame characteristics of acetone-butanol-ethanol (ABE) and toluene reference fuel (TRF) blends at atmospheric pressure. *Fuel* 232, 755–768. doi:10.1016/j.fuel.2018.05.150
- Zuo, Z. N., Hu, B., Bao, X. C., Zhang, S. B., Kong, L. G., Deng, L., et al. (2022). Quantitative research on cellular instabilities of premixed C1-C3 alkane-air mixtures using spherically expanding flames. *Fuel Process Technol.* 226, 107075. doi:10.1016/j.fuproc.2021.107075